Transition Moment Directions in Amide Crystals

Robert W. Woody,*,† Gerhard Raabe,‡ and Jörg Fleischhauer‡

Department of Biochemistry and Molecular Biology, Colorado State University, Fort Collins, Colorado 80523, and Institut für Organische Chemie, Rheinisch-Westfälische Technische Hochschule Aachen, Prof.-Pirlet-Strasse 1, D-52074 Aachen, Germany

Received: March 8, 1999; In Final Form: August 16, 1999

Transition moment directions of chromophores are critical for predicting CD and absorption spectra of biological macromolecules. Single-crystal polarized reflection spectra of a primary amide (propionamide, PrN) and a secondary amide (*N*-acetylglycine, NAG) were recently analyzed, yielding transition moment directions for the first (NV_1) and second (NV_2) $\pi\pi^*$ transitions (Clark, L. *J. Am. Chem. Soc.* **1995**, *117*, 7974). In terms of the angle θ, measured from the C═O bond with the C−N bond at positive θ, the directions for the NV_1 transitions are −37° for PrN and −55° for NAG. INDO/S MO calculations on the isolated molecules give NV_1 transition moment directions of −25° and −36° for PrN and NAG, respectively. When the mixing of excited states due to the crystal field and the exciton effect are considered, the calculated angles are −35° and −42°, respectively. For the NV_2 transitions, the angles (experiment for crystal, theory for free molecule, theory for molecule in crystal) are 46, 59, 49° for PrN and 61, 53, 55° for NAG. The present results are compared with recent ab initio results. It is proposed that the best results may be obtained by combining ab initio transition moment directions for the isolated molecule with the gas-to-crystal shift calculated by the present semiempirical method. Simplified charge models have been developed that give results for crystals of NAG essentially equivalent to those obtained with the detailed charge model. The method used in the prediction of the CD and absorption spectra of polypeptides for calculating the mixing of excited states under the influence of a static field was tested on crystals of NAG with satisfactory results. Calculations for an amide group in the middle of a 21-peptide α-helix give $\theta = -42°$ for the NV_1 transition.

Introduction

The amide group is the most abundant chromophore in polypeptides and proteins and dominates their far-ultraviolet spectra. To understand and predict the far-UV absorption and circular dichroism (CD) spectra of polypeptides and proteins, it is necessary to characterize the amide chromophore fully.

Spectroscopic studies of the amide chromophore have been comprehensively reviewed by Robin[1,2] and Clark.[3] Robin[1] proposed the currently accepted interpretation of amide gas-phase spectra. Transitions to five excited states are observed in the gas phase: $n\pi_3^*$, R_1, $\pi_2\pi_3^*$ (NV_1), R_2, $\pi_1\pi_3^*$ (NV_2), in order of increasing energy. Here π_1, π_2, and π_3^* are the π orbitals of the amide group, numbered in order of increasing energy, and R_1 and R_2 are transitions from the n and π_2 orbitals to 3s-like and 3p-like Rydberg orbitals, respectively. Thus, R_1 and R_2 do not correspond to single excited states but represent a collection of similar excited states of comparable energy. In condensed phases, the Rydberg transitions are generally not observed due to broadening and/or shifting to much higher energies, so the spectrum should simplify to a three-band spectrum, in which only the two lowest energy transitions, $n\pi^*$ and NV_1, are accessible to study in aqueous solution. However, Clark[3] has proposed that several weak bands observed in amide crystals result from Rydberg transitions.

The recent work of Clark[3] has provided critically important data on the absorption properties of primary (propionamide, PrN) and secondary (*N*-acetylglycine, NAG) amides, the structures of which are shown in Figure 1. Using polarized reflection spectroscopy on single crystals, Clark determined the transition moment directions for the first $\pi\pi^*$ transition (NV_1) of these amides. Prior to this study, only one complete determination of an amide transition moment had been reported: that of the primary amide myristamide.[4] Clark also established the transition energy, oscillator strength, and transition moment direction for the second $\pi\pi^*$ transition (NV_2) in these amides and located and characterized the NV_1 transition in the carboxyl chromophore of NAG.

Previous studies[5−7] have shown that the local electrostatic fields in a crystal can significantly modify the transition moment directions of polar chromophores, such as amides, purines, and pyrimidines, as can mixing of excited states due to exciton coupling in the crystal. The data of Clark[3] provide an important test of the methods developed to predict transition parameters in crystals.

Pajcini et al.[8] have determined the NV_1 transition moment direction in a different secondary amide crystal, glycylglycine, using polarized resonance Raman spectroscopy. The transition moment direction they obtained, $-46 \pm 3°$, may not be significantly different from the value of $-55 \pm 5°$ reported by Clark[3] for NAG. However, the difference could reflect different crystalline environments, at least in part. In any case, it is clear that secondary amides have NV_1 transition moment directions that are more negative by 10−20° than those for primary amides (−37° for propionamide[3]).

Mixing of excited states within a chromophore is one of the important mechanisms by which chromophores that are achiral

* Address correspondence to this author. Tel: 970-491-6214. Fax 970-491-0494. E-mail: rww@lamar.colostate.edu.
† Colorado State University.
‡ Rheinisch-Westfälische Technische Hochschule Aachen.

10.1021/jp990806p CCC: $18.00
Published on Web 10/04/1999

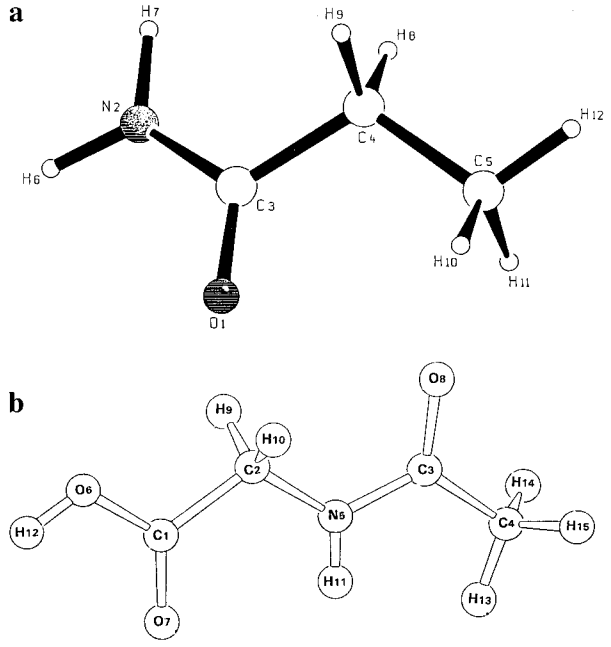

Figure 1. Structures of propionamide (a) and *N*-acetylglycine (b), showing the numbering system used in this paper.

in isolation, e.g., amides, contribute to the optical activity of chiral polymers, such as polypeptides and proteins. This mechanism is the basis of the one-electron mechanism of Condon et al.[7] and is an important element of the quantum mechanical methods currently used for calculating the CD and absorption spectra of macromolecules.[10,11] It is important to assess whether the relatively simple methods[12−15] used in these calculations can reproduce the principal effects predicted by the much more elaborate methods applicable to crystals of small molecules,[6] which are impractical for complex macromolecules with no symmetry. The data of Clark[3] provide an opportunity to test these methods and, perhaps, to develop even simpler models.

Early ab initio calculations on amide excited states[16−19] were generally limited to the simplest amide, formamide, and have been reviewed.[1,2,20] One early study[21] of *N*-methylacetamide gave transition energies and oscillator strengths, but no transition moment directions were reported. Several ab initio studies of amide chromophores have recently appeared.[20,22−27] Among these, high-level ab initio calculations (CASSCF and CASPT2) were reported for propionamide[24] and for *N*-acetylglycine,[25] the subjects of the present study. These calculations were for the isolated molecules and will be compared with the semiempirical INDO/S results for the same isolated molecules in the present work.

Methods

MO calculations were performed for propionamide and *N*-acetylglycine, using the INDO/S method of Ridley and Zerner.[28] The geometries used were taken from the crystal structures,[29−31] except for those of the hydrogens, which were placed by assuming standard bond lengths and angles. The molecular coordinates are given in Tables 1S and 2S (see Supporting Information).

For PrN, configuration interaction included 180 singly excited configurations formed from the 15 filled orbitals and the 12 empty orbitals. For NAG, 196 singly excited configurations were formed from the 14 highest filled orbitals and the 14 lowest empty orbitals.

The ground-state charge distribution of the molecules was represented by point charges at each atomic center that were calculated from the diagonal elements of the bond order matrix, taking the INDO/S wave functions to be Löwdin[32] orthogonalized orbitals. For each first-row atom, s → p hybridization moments were approximated by a pair of point charges of opposite sign placed along each coordinate axis at $\pm^{5}/_{3}\zeta^{-1}$ au from the nucleus, where ζ is the Slater orbital exponent. The charges of these sp monopoles were $\pm 3^{1/2}/4$ au, multiplied by the appropriate MO coefficients.

All ab initio calculations were carried out at the SCF level and employed the Gaussian 94 suite of quantum chemical routines[33] running on a cluster of workstations at the computing center of RWTH Aachen. Two sets of contracted Gaussian functions (6-31+G* and 6-31++G**) were used to calculate the dipole moments. Both sets of functions are based upon the standard valence double-ζ 6-31G representation,[34,35] which was supplemented by one set of diffuse (+)[36,37] s- and p- as well as d-like polarization functions (*)[38,39] on heavy atoms to yield the 6-31+G* basis set. Addition of a single set of p-type polarization functions and s-type diffuse functions to all hydrogens resulted in the 6-31++G** set, which is the largest basis used in this study.

All of the point charges for the molecule were multiplied by a scaling factor chosen to bring the dipole moment into agreement with the ab initio dipole moment for propionamide (4.46 D) and *N*-acetylglycine (2.79 D), using a high-level basis set (6-31++G**). These scaling factors were 0.807 (PrN) and 0.871 (NAG). The scaled charges were placed on all the molecules within eight unit cells in each direction, thus including 19 651 molecules. The electrostatic potential and electric field were calculated at each atom of the central molecule, using these point charges. Tests showed that increasing the number of unit cells included in the calculation from eight in each direction to fourteen in each direction had no significant effect on the final results; i.e., changes of less than 0.1% in the calculated transition parameters were obtained.

The potentials and fields calculated as described were included in the Fock matrix for the INDO/S calculation.[6] The modified Fock matrix elements are

$$\mathbf{F}_{\mu\mu} = \mathbf{F}_{\mu\mu}{}^{0} - V_{\mathrm{a}} \tag{1}$$

$$\mathbf{F}_{\mu\nu} = \mathbf{F}_{\mu\nu}{}^{0} + \mathbf{E}_{\mathrm{a}}\cdot\mathbf{r}_{\mu\nu} \tag{2}$$

where $\mathbf{F}_{\mu\mu}{}^{0}$ and $\mathbf{F}_{\mu\nu}{}^{0}$ are respectively the diagonal and off-diagonal Fock matrix elements in the absence of the field, V_{a} is the electrostatic potential at atom a on which orbital μ is located, $\mathbf{E}_{\mathrm{a}}$ is the electric field at atom a, and $\mathbf{r}_{\mu\nu}$ is the matrix element of the position operator connecting orbitals μ and ν, which vanishes unless μ = 2s and ν = 2p or vice versa.

The process was iterated, with new ground-state charges, fields, and potentials calculated in each round, until the electron energy converged to within 10^{-6} au. This required nine iterations for PrN and eight for NAG. The transition parameters converged to within 1 ppm in five or six iterations.

Exciton splitting[40] causes each transition of the isolated molecule to split into Z levels, where Z is the number of molecules per unit cell. Of these, only one, two, or three, depending on the unit cell symmetry, are connected to the ground state by electric-dipole-allowed transitions. Both amide crystals belong to the $P2_1/c$ space group with four molecules per unit cell and each molecular transition gives rise to one allowed transition polarized along the *b* axis and another in the *ac* plane.

Intermolecular interactions were treated as perturbations, according to the methods of Craig and Walmsley,[40] as described previously.[7] The transition charge densities were approximated by transition monopoles that were placed on all the molecules within four unit cells in each direction, thus including 2915 molecules.

Closely spaced transitions were combined by summing the squares of the components of their transition moments along the three crystal axes. After taking the square roots, the components were combined with all possible choices of relative sign (four independent choices) and then transformed from the crystal coordinate system into the molecular coordinate system. In most cases, two of these choices were polarized, to a good approximation, in the plane of the amide (or carboxyl) group, corresponding to the two alternative polarization directions for $\pi\pi^*$ transitions. In a few cases, all four combinations had significant out-of-plane components. These were interpreted as $n\pi^*$ transitions and are denoted as such in the tabulated results.

In the matrix method,[11] the most widely used method for calculating the CD spectra of polypeptides and proteins, mixing of excited states within a chromophore is calculated by diagonalizing a matrix, the diagonal elements of which are the transition energies of the chromophore in the crystal field. (The transition energies of the isolated molecule, calculated or experimental, have generally been used for these diagonal matrix elements, but in the present case, the effects of the local electrostatic environment on the transition energy are considered.) The off-diagonal elements are the Coulombic interaction between the transition density connecting the pair of excited states and the ground-state charge densities of the surrounding groups. In the present calculation, point charges at the atoms and along the coordinate axes were used, as previously described, to calculate the potential, field, and field gradient at each atom of the molecule under consideration. (The field gradient is important in the present context because transition quadrupoles are the lowest order of allowed multipoles for transitions connecting $n\pi^*$ and $\pi\pi^*$ states or the ground state and $n\pi^*$ states.) The potentials, fields, and field gradients at each center were combined with point monopoles, dipoles, and quadrupoles, respectively, calculated for the transition density at each center from the INDO/S wave functions for the isolated molecule. The off-diagonal element connecting states α and β, $V_{\alpha\beta}$, is given by

$$V_{\alpha\beta} = \sum_a (V_a q_{\alpha\beta a} - \mathbf{E}_a \cdot \mu_{\alpha\beta a} - {}^1/_6 \mathbf{E}_a' : \mathbf{Q}_{\alpha\beta a}) \qquad (3)$$

where V_a and $\mathbf{E}_a$ are as defined in eqs 1 and 2; $\mathbf{E}_a'$ is the field-gradient tensor at center a; $q_{\alpha\beta a}$, $\mu_{\alpha\beta a}$, and $\mathbf{Q}_{\alpha\beta a}$ are respectively the point monopole, point dipole moment, and point quadrupole tensor for the transition $\alpha \rightarrow \beta$ at center a; and the double dot product of two vectors, **a** and **b**, is defined as $\mathbf{a:b} = \bar{Z}_i \bar{Z}_j a_{ij} b_{ji}$.

The diagonal elements of the matrix, $V_{\alpha\alpha}$, are given by

$$V_{\alpha\alpha} = E_{\alpha\alpha}{}^0 + \sum_a [V_a (q_{\alpha\alpha a} - q_{00a}) - \mathbf{E}_a \cdot (\mu_{\alpha\alpha a} - \mu_{00a}) - {}^1/_6 \mathbf{E}_a' : (\mathbf{Q}_{\alpha\alpha a} - \mathbf{Q}_{00a})] \qquad (4)$$

where the subscripts α and 0 refer respectively to the excited-state and ground-state charge distributions. These moments were also calculated from the INDO/S wave functions of the isolated molecule, and are scaled with the same scaling factor used for the ground-state charges, as described previously. No scaling factors were applied to the transition dipole moments.

The eigenvalues of the **V** matrix represent the transition energies of the chromophore in the static field of the crystal.

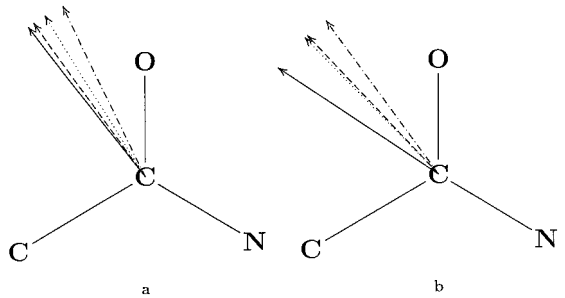

Figure 2. NV_1 transition moment directions in (a) PrN and (b) NAG. The solid arrow is Clark's[3] experimental direction for the crystal; the arrow with alternating dashes and dots is the INDO/S direction for the isolated molecule; the arrow with dots is the ab initio direction for the isolated molecule;[24,25] the arrow with dashes is the INDO/S direction for the crystal. For NAG, the ab initio direction for the isolated molecule and the INDO/S direction for the crystal are within 1° of each other, so they are difficult to distinguish.

The eigenvectors are the coefficients describing the mixing of the excited states and can be used to calculate the electric dipole transition moments from the ground state to the excited states in the crystal field. From these, the transition moment directions and the oscillator strengths are obtained.

A model using three transitions ($n\pi^*$, NV_1, and NV_2) and monopoles at five centers (C, H, O, and N of the amide and one of the C_α's) was used to calculate the spectroscopic parameters of a peptide group in the α-helix. INDO/S wave functions for NMA were used, together with the methods applied to the PrN and NAG crystals described above. Atomic coordinates for the 21-residue helix were generated by matrix transformations[41] of the standard trans peptide geometry of Momany et al.[42] using $(\phi, \psi) = (-62°, -41°)$, found by Barlow and Thornton[43] as the average Ramachandran[44] angles for α-helices in a set of 57 proteins. The potentials, fields, and field gradients at the atoms of the central residue were calculated. In the central residue and all residues following it, the charges of the *N*-methyl group and the hydrogens of the *C*-methyl group of NMA were set to zero, distributing the residual charge so that the changes in charge were minimal in the least-squares sense and the dipole moment of the molecule was conserved.[45] Peptide groups N-terminal to the central residue were treated similarly, except that the *C*-methyl group and the hydrogens on the *N*-methyl group were assigned zero charge. This procedure avoids problems that would otherwise occur because the peptide groups share C_α atoms.

Results and Discussion

The experimental NV_1 transition moments determined by Clark[3] for PrN and NAG are represented in Figure 2, in comparison with those calculated for these molecules in the gas phase (isolated) by INDO/S. The difference between the directions is 12° for PrN and 20° for NAG. Clark also performed INDO/S calculations on these two molecules, and our results agree. Clark's experimental value for PrN agrees well with that of Peterson and Simpson[4] for myristamide. It should be noted that nearly all earlier theoretical calculations for peptide optical properties[11−14,46] used the Peterson and Simpson value, and Clark's work shows that this is 15−20° different from the value for a secondary amide.

The dipole moment magnitudes and directions obtained from INDO/S and several ab initio basis sets are shown in Tables 1 (PrN) and 2 (NAG). Tables 3 and 4 show the atom-centered charges calculated for the atoms of PrN and NAG, respectively, in their ground states, both as isolated molecules and in the crystal. The charges on the sp monopoles are given in Tables

TABLE 1: Ground-State Dipole Moments for Propionamide

		$\|\mu\|$ (D)	θ^a (deg)
	Gas Phase		
ab initio	6-31+G*	4.48	173
	6-31++G**	4.46	173
INDO/S	unscaled	5.52	173
	scaled[b]	4.46	173
	Crystal		
scaled INDO/S	first iteration[c]	5.29	170
scaled INDO/S	ninth iteration[d]	5.46	170

[a] Angle between ground-state dipole moment and carbonyl bond direction (C → O). Rotation toward CN bond is positive. [b] The INDO/S dipole moment is multiplied by a factor that brings its magnitude into agreement with the best ab initio dipole moment, i.e., the value from the 6-31++G** basis set. [c] Scaled gas-phase INDO/S charges were placed on the surrounding molecules. [d] After convergence, INDO/S charges were placed on the surrounding molecules.

TABLE 2: Ground-State Dipole Moments for *N*-Acetylglycine

		$\|\mu\|$ (D)	θ^a (deg)
	Gas Phase		
ab initio	6-31+G*	2.82	147
	6-31++G**	2.79	147
INDO/S	unscaled	3.21	154
	scaled[b]	2.79	154
	Crystal		
scaled INDO/S	first iteration[c]	3.83	153
scaled INDO/S	eighth iteration[d]	4.07	152

[a] Angle between ground-state dipole moment and carbonyl bond direction (C → O). Rotation toward CN bond is positive. [b] The INDO/S dipole moment is multiplied by a factor that brings its magnitude into agreement with the best ab initio dipole moment, i.e., the value from the 6-31++G** basis set. [c] Scaled gas-phase INDO/S charges were placed on the surrounding molecules. [d] After convergence, INDO/S charges were placed on the surrounding molecules.

TABLE 3: Atomic Charges and Potentials for Propionamide

atom	initial charge[a]	final charge[b]	initial potential[c]	final potential[d]
O1	−0.4890	−0.5712	0.045 14	0.055 10
N2	−0.1669	−0.1558	−0.022 47	−0.026 11
C3	0.3334	0.3477	0.007 49	0.008 97
C4	0.0188	0.0191	0.002 02	0.001 86
C5	−0.0160	−0.0144	0.017 54	0.019 94
H6	0.1303	0.1469	−0.034 00	−0.038 95
H7	0.1161	0.1533	−0.068 01	−0.078 14
H8	0.0223	0.0209	0.004 47	0.003 21
H9	0.0138	0.0248	−0.014 01	−0.015 98
H10	0.0146	0.0147	0.016 98	0.020 25
H11	0.0200	0.0120	0.028 83	0.033 35
H12	0.0025	0.0020	0.016 03	0.016 51

[a] Charge for isolated molecule (au). [b] Charge for molecule in crystal subject to potentials and fields due to charges on surrounding molecules after convergence of iterative process (au). [c] Potential at atom with charges for isolated molecule on surrounding molecules (au). [d] Potential at atom subject to potentials and fields due to charges on surrounding molecules after convergence of iterative process (au).

3S and 4S in the Supporting Information. Comparison of columns 2 and 3 in Tables 3 and 4 shows the polarizing effect of the crystal environment. The charges on the atoms in the crystal relative to those in the isolated molecule show significant increases in magnitude, especially for the polar atoms involved in hydrogen bonding, i.e., the carbonyl oxygen(s) and the amide and carboxyl hydrogens. Thus H-bond donor hydrogens become more positive and better H-bond donors, whereas H-bond acceptor oxygens become more negative and better H-bond acceptors. This polarization is also evident in the increase in

TABLE 4: Atomic Charges and Potentials for *N*-Acetylglycine

atom	initial charge[a]	final charge[b]	initial potential[c]	final potential[d]
C1	0.4299	0.4477	−0.002 72	−0.006 42
C2	0.1003	0.1031	0.006 54	0.005 84
C3	0.3564	0.3755	0.020 12	0.025 12
C4	0.0012	−0.0044	−0.000 54	0.001 61
N5	−0.1500	−0.1213	−0.004 41	−0.003 80
O6	−0.2609	−0.2822	−0.006 69	−0.012 86
O7	−0.4696	−0.5054	0.009 67	0.009 76
O8	−0.5325	−0.6369	0.070 89	0.082 30
H9	0.0477	0.0489	0.010 66	−0.008 31
H10	0.0496	0.0465	0.015 47	0.014 56
H11	0.1393	0.1696	−0.041 93	−0.037 97
H12	0.2085	0.2526	−0.054 33	−0.067 11
H13	0.0107	0.0390	−0.034 35	−0.037 84
H14	0.0351	0.0320	0.009 62	0.012 32
H15	0.0344	0.0354	0.002 00	0.006 17

[a] Charge for isolated molecule (au). [b] Charge for molecule in crystal subject to potentials and fields due to charges on surrounding molecules after convergence of iterative process (au). [c] Potential at atom with charges for isolated molecule on surrounding molecules (au). [d] Potential at atom subject to potentials and fields due to charges on surrounding molecules after convergence of iterative process (au).

the calculated dipole moments. For PrN (Table 1), consideration of the scaled gas-phase charges leads to an increase from 4.46 to 5.29 D. The converged charges lead to a dipole moment of 5.46 D in the crystal. For NAG (Table 2), the dipole moment increases from 2.79 to 3.83 and 4.07 D, respectively, upon application of the isolated molecule charges and those after convergence in the crystal.

The potentials calculated at the various atoms of PrN and NAG are shown in Tables 3 and 4, respectively. Comparison of columns 4 and 5 of these tables shows the effects of polarization in the general *increase* in the magnitude of the potentials calculated with the converged crystal charges relative to those obtained with charges for the isolated molecule. The most important parameter from these results is the potential difference across the amide group, from the carbonyl oxygen to the peptide hydrogen. This is 3.1 eV for the trans and 2.2 eV for the cis hydrogen in PrN and 2.5 eV for the trans hydrogen in NAG. Crystal polarization effects increase these potential differences by 0.5, 0.4, and 0.4 eV, respectively. The potential difference across the amide group is the principal factor leading to mixing of the excited states by the crystal field.

Table 5 compares the calculated transition parameters with those observed for PrN obtained by Clark.[3] The calculated gas-phase NV_1 transition moment direction differs by 12° from the observed direction. The crystal field rotates the direction by 10° from that for the isolated molecule toward the observed crystal direction, bringing it into good agreement with experiment. Exciton mixing of excited states has no significant effect in this case. It should be noted that a similar improvement is obtained for the NV_2 transition, but the exciton effect is more important than the crystal field mixing in this case. The $n\pi^*$ transition energy of carbonyl compounds, it should be noted, is underestimated substantially in INDO/S and CNDO/S calculations. The crystal field effect blue-shifts the $n\pi^*$ band by 45 nm, but the wavelength is still too long.

The corresponding results for NAG are shown in Table 6. The crystal field effect rotates the NV_1 transition moment direction of the secondary amide in NAG by −9°, about the same amount as in the case of the primary amide PrN. In NAG, however, the exciton effect leads to a small rotation in the positive direction, so although the results calculated for the

TABLE 5: Spectroscopic Parameters for Propionamide Crystals

	gas phase			crystal + crystal field			crystal + exciton effects			experiment[3]		
	λ^a	f^b	θ^c	λ	f	θ	λ	f	θ	λ	f	θ
nπ*	323	0.001	⊥	278	0.001	⊥	278	0.001	⊥	208	0.001	⊥
										196[d]	0.01	−38
NV_1	190	0.31	−25	193	0.32	−35	194	0.32	−35	181	0.17	−37
	160	0.01	−48	151	0.01	⊥	150	0.01	+11			
	152	0.02	⊥	148	0.01	⊥						
	147	0.02	⊥	143	0.08	+45						
NV_2	139	0.17	+59	139	0.11	+56	140	0.2	+49	127	0.1	+46

[a] Wavelength, nm. [b] Oscillator strength. [c] The angle in degrees between the transition dipole moment and the carbonyl bond direction, with positive angles toward the amide N. ⊥ denotes a transition with a significant out-of-plane transition moment, i.e., making an angle greater than 20° with respect to the amide plane. [d] Assigned by Clark[3] as a Rydberg transition and therefore not predicted by INDO/S.

TABLE 6: Spectroscopic Parameters for *N*-Acetylglycine Crystals[a]

	gas phase			crystal + crystal field			crystal + exciton effects			experiment[3]		
	λ^b	f^c	θ^d	λ	f	θ	λ	f	θ	λ	f	θ
nπ*	*317*	*0*	⊥	*289*	*0*	⊥	*289*	*0*	⊥	213	0.001	⊥
nπ*	304	0	⊥	266	0	⊥	266	0	⊥	(208[e])	0	(⊥)
										192[f]	0.01	(−55)
NV_1	195	0.3	−35	197	0.33	−44	203	0.33	−42	187	0.23	−55
CT[g]	187	0.01	−39	175	0.02	−40	175	0.02	−42	*179*[h]	*0.01*	*4 or −55*
NV_1	*159*	*0.15*	*−25*	*160*	*0.29*	*−17*	*160*	*0.3*	*−43, −13*	*156*	*0.17*	*0 or −57*
	158	*0.13*	*+6*									
NV_2	138	0.18	53	139	0.21	+48	140	0.26	15 or 55	139	0.1	10 or 61

[a] Entries in italics refer to the carboxyl chromophore in NAG. Other entries refer to the secondary amide chromophore. [b] Wavelength, nm. [c] Oscillator strength. [d] The angle in degrees between the transition dipole moment and the carbonyl bond direction, with positive angles toward the amide N. ⊥ denotes a transition with a significant out-of-plane transition moment, i.e., making an angle greater than 20° with respect to the amide plane. The values in italics refer to carboxyl group transitions and are defined in an analogous way for this group. [e] Entries in parentheses were inferred by Clark[3] and not actually observed. [f] Assigned by Clark[3] as a Rydberg transition and therefore not predicted by INDO/S. [g] A charge-transfer transition (amide → carboxyl) is predicted by INDO/S. An experimental feature in this region was assigned by Clark[3] as a Rydberg transition in the carboxyl group (see footnote *h*). [h] Assigned as a Rydberg transition by Clark[3] but consistent with a predicted band.

crystal are substantially better than those for the isolated molecule, there is a significant residual discrepancy of 13°. The amide NV_2 transition moment is rotated away from the experimental direction by crystal field effects, but this is reversed by the exciton effect, with a small net improvement in agreement with experiment. The carboxyl NV_1 transition shows a larger residual discrepancy, 13−14°, comparable to that for the amide NV_1. Nonetheless, this is a significant improvement over the gas-phase result, which differs by ∼25−30°.

One of the weak transitions predicted by INDO/S for NAG is of interest. This is predicted at 187 nm for the isolated molecule, with an oscillator strength of 0.01 and a polarization close to that of the NV_1 transition. Examination of the MO coefficients and changes in charge density upon excitation show that it is a charge-transfer transition, primarily from the highest filled π orbital of the amide group to the empty π* orbital of the carboxyl. The crystal field causes this transition to blue-shift to 175 nm and double in intensity, but exciton interactions have little effect on the transition. Clark[3] observed a band with appropriate intensity and polarization at 179 nm in the crystal spectrum of NAG but assigned it to a Rydberg transition in the carboxyl group, analogous to the Rydberg transition assigned on the long-wavelength side of the amide NV_1 band. Because INDO/S does not include Rydberg-type orbitals in the basis set, our calculations cannot provide support for or against the Rydberg assignment of the 179 nm band. They do, however, suggest that the band could be due, at least in part, to a charge-transfer transition.

Charge-transfer bands were predicted by ab initio calculations[25] on NAG at 176 nm, $f = 0.033$, and at 173 nm, $f = 10^{-4}$. The former is a transition from amide π_2 to carboxyl π_3*, corresponding to the INDO/S result, and the latter is from the n orbital of the carboxyl to the π_3* orbital of the amide. Serrano-Andrés and Fülscher[25,26] have found amide−amide charge-transfer transitions in ab initio calculations on several di- and tripeptides at about 1 eV above the NV_1 transitions.

Experimental evidence from resonance Raman excitation spectra for relatively low-energy charge-transfer transitions in related systems has been reported by Asher and co-workers,[8,47] who observed transitions from the terminal carboxylate groups to peptide groups in a number of amino acid derivatives. These transitions are observed just to the red of the NV_1 transition, consistent with the lower ionization potential for the ionized carboxyl group.

Table 7 compares the results of the INDO/S calculations for the isolated propionamide and NAG molecules with ab initio results.[24,25] Only valence-shell transitions are shown from the ab initio method, since Rydberg orbitals are not included in the basis set for INDO/S. As expected, the ab initio transition energies of the nπ* transitions are in much better agreement with experiment (cf. Tables 5 and 6) than those from INDO/S. The INDO/S calculations also underestimate the transition energies for other valence-shell transitions, although not as markedly as for the nπ* transitions. The oscillator strengths from the two methods generally agree satisfactorily. The transition moment directions also show rather good agreement for the amide NV_1 transition, differing by 6−8°. In both amides, the ab initio direction is more negative than the INDO/S value, yielding a smaller discrepancy with the experimental solid-state direction. INDO/S calculations have also been performed (data not shown) for other simple amides for which ab initio transition moment directions have been reported.[20,22,24] In all cases,

TABLE 7: Comparison of ab initio and INDO/S Results for the Gas Phase[a]

	ab initio[24,25]			INDO/S			experiment (crystal)[3]		
	λ[b]	f[c]	θ[d]	λ	f	θ	λ	f	θ
				Propionamide					
nπ*	226	0.001	$\perp$	323	0.001	$\perp$	208	0.001	$\perp$
NV_1	170	0.346	−31	190	0.31	−25	181	0.17	−35[e]
NV_2	125	0.205	+52	139	0.17	+59	127	0.1	+46
				N-Acetylglycine					
*nπ**	*236*	*0.001*	$\perp$	*317*	*0*	$\perp$	(*208*)	(*0.001*)	$\perp$
nπ*	220	0.001	$\perp$	304	0	$\perp$	213	0.001	$\perp$
NV_1	183	0.292	−43	195	0.3	−35	187	0.23	−55
CT	176	0.033	−25	187	0.01	−39	*179*	*0.01*	*4 or −55*
NV_1	*145*	*0.35*	*−2*	*159*	*0.15*	*−25*	*156*	*0.17*	*4 or −61*
				158	*0.13*	*+6*			
NV_2	130	0.125	+28	138	0.18	+53	139	0.1	10 or 61

[a] Only valence-shell transitions from the ab initio results are given, since the INDO/S calculations do not include Rydberg orbitals in the basis set. [b] Wavelength, nm. [c] Oscillator strength. [d] The angle in degrees between the transition dipole moment and the carbonyl bond direction, with positive angles toward the amide N. $\perp$ denotes a transition polarized perpendicular to the amide plane. Values in italics refer to carboxyl group transitions and are defined analogously to those for the amide group. Note that Serrano-Andrés and Fülscher[25] used the carboxyl group of *N*-acetylglycine as the reference for both amide and carboxyl transitions. Their values for amide transitions have been converted to our convention. The transition at 176 nm in ab initio and at 187 nm in INDO/S is a charge-transfer transition, and θ is defined relative to the amide group. [e] This is the direction in the model spectrum, corrected for intermolecular interactions in the crystal, and differs by 2° from the observed direction (−37°).

INDO/S gives an NV_1 transition moment that is less negative than the ab initio result, with differences ranging from 2 to 6°. The amide NV_2 transition moment directions show the largest discrepancies, with differences of 13° for PrN and 25° for NAG. In the former case, the ab initio value for the isolated molecule is only 6° away from the experimental crystal value, but in the latter case, the discrepancy is 18° or 33°, depending on which of the possible experimental values is correct.

The INDO/S calculations reported here do not give values for the transition moment directions in the isolated molecules that agree as well with the crystal directions as do the ab initio calculations[24,25] for isolated molecules. As noted above, INDO/S systematically underestimates the angle between the NV_1 transition moment and the carbonyl bond direction for amides relative to ab initio calculations. The predicted *shifts* on going from the isolated molecule to the crystal are likely to be accurate within a few degrees, however. If the INDO/S-calculated shifts are combined with the ab initio predictions for the isolated molecules, the NV_1 transition moment directions are −41° and −50° for PrN and NAG, respectively, as compared with −37° and −55° observed experimentally. These values are in as good as or better agreement than the uncorrected ab initio values. In the case of the NV_2 transition, this approach works well for PrN (+42° corrected ab initio vs +46° observed) but not for NAG (+30° corrected ab initio vs +60° or +10°). In this case, as noted above, the ab initio NV_2 shows an unusually large discrepancy with experiment, larger than the INDO/S result, and because of the high energy of this transition, there are larger uncertainties in both theory and experiment.

Table 8 shows a comparison of the predicted crystal spectroscopic parameters for NAG obtained with the crystal field method just described and the substantially simpler matrix method, comparable to that used in calculations of polypeptide CD spectra. The full charge model uses the same set of charges on the surrounding molecules and so is directly comparable. It can be seen that the results are very similar, except for those of the NV_2 transition, which is the highest energy transition considered in the matrix method and therefore is affected by the truncation of the basis set.

TABLE 8: Spectroscopic Parameters from Complete and Simplified Models for NAG

			matrix method								
crystal field			full charge model			simplified model			three transitions		
λ[a]	f[b]	θ[c]	λ	f	θ	λ	f	θ	λ	f	θ
289	*0*	$\perp$	*290*	*0*	$\perp$	*290*	*0*	$\perp$			
266	0	$\perp$	257	0	$\perp$	257	0	$\perp$	256	0	$\perp$
197	0.33	−44	203	0.28	−46	201	0.28	−46	201	0.28	−43
175	0.02	−42	175	0.02	−40	179	0.02	−36			
160	*0.29*	*−17*	*160*	*0.29*	*−17*	*157*	*0.26*	*−13*			
140	0.21	48	135	0.27	+32	135	0.27	32	133	0.20	35

[a] Wavelength, nm. [b] Oscillator strength. [c] The angle in degrees between the transition dipole moment and the carbonyl bond direction, with positive angles toward the amide N. $\perp$ denotes a transition with a significant out-of-plane transition moment, i.e., making an angle greater than 20° with respect to the amide plane. The values in italics refer to carboxyl group transitions and are defined in an analogous way for this group.

TABLE 9: Atomic Charges and Potentials for the Simplified *N*-Acetylglycine Model

atom	full charge[a]	simple charge[b]	full potential[c]	simple potential[d]
C1	0.4299	0.4374	−0.0269	−0.0210
C2	0.1003	0.0	−0.0176	−0.0125
C3	0.3564	0.4536	−0.0036	−0.0040
C4	0.0012	0.0	−0.0238	−0.0260
N5	−0.1500	−0.0574	−0.0284	−0.0264
O6	−0.2609	−0.2277	−0.0304	−0.0259
O7	−0.4696	−0.5117	−0.0154	−0.0093
O8	−0.5325	−0.4891	0.0466	0.0464
H9	0.0477	0.0	−0.0143	−0.0092
H10	0.0496	0.0	−0.0088	−0.0026
H11	0.1393	0.1532	−0.0630	−0.0632
H12	0.2085	0.2416	−0.0769	−0.0696
H13	0.0107	0.0	−0.0576	−0.0605
H14	0.0351	0.0	−0.0132	−0.0161
H15	0.0344	0.0	−0.0214	−0.0240

[a] Charge (au) for isolated molecule. [b] Charge (au) for simplified charge model. Charges on alkyl carbons and hydrogens are set to zero. Charges on remaining atoms are adjusted to preserve neutrality and the dipole moment (see Methods). [c] Potential (au) at atom resulting from placing charges from full charge model on surrounding molecules. These potentials differ from those given in Table 4 because the sp charges were not used in this calculation. [d] Potential (au) at atom resulting from placing charges from simplified charge model on surrounding molecules.

The test of a simplified charge model gives encouraging results. Eliminating all charges on the methylene and methyl atoms of NAG and adjusting charges on the remaining atoms while preserving the neutrality and the dipole moment of the full molecule give the set of charges shown in Table 9. Although there are some significant changes in charges on the polar atoms retained in the model, the potentials calculated with this streamlined model show relatively small differences from those obtained with all of the charges (Table 9). In Table 8, it can be seen that the simplified model gives transition parameters that differ insignificantly from those obtained by the matrix method using the full set of charges. Finally, the last three columns of Table 8 illustrate that consideration of only three excited states (nπ*, NV_1, and NV_2) in the secondary amide gives results equivalent to those obtained with the 15 lowest energy excited states of NAG.

TABLE 10: Spectroscopic Parameters for an Amide in an α-Helix

	gas phase			α-helix		
	λ^a	$\|\mu\|^b$	θ^c	λ	$\|\mu\|$	θ
nπ*	313	0.23	⊥	287	0.37	−25
NV_1	196	3.52	−35	198	3.50	−42
NV_2	136	2.39	+44	133	2.17	+37

[a] Wavelength, nm. [b] Transition dipole moment magnitude, D. [c] The angle in degrees between the transition dipole moment and the carbonyl bond direction, with positive angles toward the amide N. ⊥ denotes a transition polarized perpendicular to the amide plane.

Table 10 shows the results of using the simplified-charge, three-transition model to calculate transition parameters for a peptide in the middle of an α-helix. As expected, the nπ* transition undergoes a substantial blue shift due to the crystal field of the helix. This field also mixes the nπ* and $\pi\pi$* transitions, leading to a 2.5-fold increase in dipole strength and an in-plane component that is stronger than the intrinsic out-of-plane component. The main effect of the crystal field on the NV_1 transition is to rotate the transition moment by 7° away from the carbonyl bond direction, so that the direction is closer to that observed by Clark[3] for NAG. In fact, the crystal-field effect we calculate for NMA in the α-helix is comparable to that we predict for the secondary amide in the NAG crystal. The crystal-field effect on the NV_2 transition moment direction in the α-helix is also comparable to that predicted for NAG crystals.

Conclusions

Semiempirical MO theory, modified to include crystal field effects and combined with exciton calculations, gives an excellent account of the transition moment directions in propionamide crystals and reasonably satisfactory results for *N*-acetylglycine. The combined effects of crystal fields and exciton mixing lead to changes in transition moment direction of the order of 10° on going from the isolated molecule to the crystal. In all cases studied here, the change in orientation leads to improved agreement with experiment. The best results may be obtained by combining ab initio calculations for the isolated molecule with gas-to-crystal shifts calculated by the semiempirical methods used here.

The matrix method for calculating mixing of excited states within a chromophore due to the electrostatic environment gives results that agree well with those obtained by the much more elaborate method in which the potentials and fields are incorporated in the semiempirical Hamiltonian.

The matrix method calculations can be simplified by considering only charges at polar atoms, with little loss in accuracy. The properties of the three principal excited states of the secondary amide (nπ*, NV_1, and NV_2) in *N*-acetylglycine can be predicted satisfactorily in a model in which other excited states of the molecule are neglected. The same model predicts that comparable crystal-field effects occur in the α-helix.

Acknowledgment. We thank Prof. Axel Wollmer, Institut für Biochemie, RWTH Aachen, for stimulating discussions. Dr. N. Sreerama, Colorado State University, made important contributions to several of the programs used in these calculations. R.W.W. gratefully acknowledges financial support from the NIH, in the form of a Fogarty Senior International Fellowship (TW02122) and a research grant (GM22994), and from Colorado State University, in the form of a sabbatical leave.

Supporting Information Available: Tables 1S−4S, listing coordinates for propionamide, coordinates for *N*-acetylglycine, charges for sp monopoles on propionamide, and charges for sp monopoles on *N*-acetylglycine. This material is available free of charge via the Internet at http://pubs.acs.org.

References and Notes

(1) Robin, M. B. *Higher Excited States of Polyatomic Molecules*; Academic Press: New York, 1974; Vol. 2, pp 122−160.
(2) Robin, M. B. *Higher Excited States of Polyatomic Molecules*; Academic Press: Orlando, FL, 1985; Vol. 3, pp 303−308.
(3) Clark, L. B. *J. Am. Chem. Soc.* **1995**, *117*, 7974.
(4) Peterson, D. L.; Simpson, W. T. *J. Am. Chem. Soc.* **1955**, *77*, 3929; **1957**, *79*, 2375.
(5) Woody, R. W. *Federation of European Chemical Societies International Conference on Circular Dichroism*, Conference Proceedings; Bulgarian Academy of Sciences: Sofia, Bulgaria, 1985; Vol. 6, pp 270−295.
(6) Theiste, D.; Callis, P. R.; Woody, R. W. *J. Am. Chem. Soc.* **1991**, *113*, 3260.
(7) Sreerama, N.; Woody, R. W.; Callis, P. R. *J. Phys. Chem.* **1994**, *98*, 10397.
(8) Pajcini, V.; Chen, X. G.; Bormett, R. W.; Geib, S. J.; Li, P.; Asher, S. A.; Lidiak, E. G. *J. Am. Chem. Soc.* **1996**, *118*, 9716.
(9) Condon, E. U.; Altar, W.; Eyring, H. *J. Chem. Phys.* **1937**, *5*, 753.
(10) Tinoco, I., Jr. *Adv. Chem. Phys.* **1962**, *4*, 113.
(11) Bayley, P. M.; Nielsen, E. B.; Schellman, J. A. *J. Phys. Chem.* **1969**, *73*, 228. Goux, W. J.; Hooker, T. M., Jr. *J. Am. Chem. Soc.* **1980**, *102*, 7080.
(12) Schellman, J. A.; Oriel, P. J. *J. Chem. Phys.* **1962**, *37*, 2114.
(13) Woody, R. W.; Tinoco, I., Jr. *J. Chem. Phys.* **1967**, *46*, 4927.
(14) Woody, R. W. *J. Chem. Phys.* **1968**, *49*, 4797.
(15) Kurapkat, G.; Krüger, P.; Wollmer, A.; Fleischhauer, J.; Kramer, B.; Zobel, E.; Koslowski, A.; Botterweck, H.; Woody, R. W. *Biopolymers* **1997**, *41*, 267.
(16) Basch, H.; Robin, M. B.; Kuebler, N. A. *J. Chem. Phys.* **1967**, *47*, 1201.
(17) Harding, L. B.; Goddard, W. A. *J. Am. Chem. Soc.* **1975**, *97*, 6300.
(18) Stenkamp, L. Z.; Davidson, E. R. *Theor. Chim. Acta* **1977**, *44*, 405.
(19) Oliveros, E.; Riviere, M.; Teichteil, C.; Malrieu, P. *Chem. Phys. Lett.* **1978**, *57*, 220.
(20) Hirst, J. D.; Hirst, D. M.; Brooks, C. L., III. *J. Phys. Chem.* **1996**, *100*, 13487.
(21) Nitzsche, L. E.; Davidson, E. R. *J. Am. Chem. Soc.* **1978**, *100*, 7201.
(22) Hirst, J. D.; Hirst, D. M.; Brooks, C. L., III. *J. Phys. Chem. A* **1997**, *101*, 4821.
(23) Hirst, J. D.; Persson, B. J. *J. Phys. Chem. A* **1998**, *102*, 7519.
(24) Serrano-Andrés, L.; Fülscher, M. P. *J. Am. Chem. Soc.* **1996**, *118*, 12190.
(25) Serrano-Andrés, L.; Fülscher, M. P. *J. Am. Chem. Soc.* **1996**, *118*, 12200.
(26) Serrano-Andrés, L.; Fülscher, M. P. *J. Am. Chem. Soc.* **1998**, *120*, 10912.
(27) Besley, N. A.; Hirst, J. D. *J. Phys. Chem. A* **1998**, *102*, 10791.
(28) Ridley, J.; Zerner, M. *Theor. Chim. Acta* **1973**, *32*, 111.
(29) Carpenter, G. B.; Donohue, J. *J. Am. Chem. Soc.* **1950**, *72*, 2315.
(30) Donohue, J.; Marsh, R. E. *Acta Crystallogr.* **1962**, *15*, 941.
(31) Usanmaz, A.; Adler, G. *Acta Crystallogr.* **1982**, *B38*, 660.
(32) Löwdin, P. O. *J. Chem. Phys.* **1950**, *18*, 365.
(33) Frisch, M. J.; Trucks, G. W.; Schlegel, H. B.; Gill, P. M. W.; Johnson, B. G.; Robb, M. A.; Cheeseman, J. R.; Keith, T. A.; Petersson, G. A.; Montgomery, J. A.; Ragavachari, K.; Al-Laham, M. A.; Zakrzewski, V. G.; Ortiz, J. V.; Foresman, J. B.; Cioslowski, J.; Stefanov, B. B.; Nanayakkara, A.; Challacombe, M.; Peng, C. Y.; Ayala, P. Y.; Chen, W.; Wong, M. W.; Andres, J. L.; Replogle, E. S.; Gomperts, R.; Martin, R. L.; Fox, D. J.; Binkley, J. S.; Defrees, D. J.; Baker, J.; Stewart, J. P.; Head-Gordon, M.; Gonzalez, C.; Pople, J. A. *Gaussian94*, Revision D.4; Gaussian, Inc.: Pittsburgh, PA, 1995.
(34) Ditchfield, R.; Hehre, W. J.; Pople, J. A. *J. Chem. Phys.* **1971**, *54*, 724.
(35) Hehre, W. J.; Ditchfield, R.; Pople, J. A. *J. Chem. Phys.* **1972**, *56*, 2257.

(36) Clark, T.; Chandrasekhar, J.; Spitznagel, G. W.; Schleyer, P. v. R. *J. Comput. Chem.* **1983**, *4*, 294.
(37) Frisch, M. J.; Pople, J. A.; Binkley, J. S. *J. Chem. Phys.* **1984**, *80*, 3265.
(38) Hariharan, P. C.; Pople, J. A. *Theor. Chim. Acta* **1973**, *28*, 213.
(39) Hariharan, P. C.; Pople, J. A. *Mol. Phys.* **1974**, *27*, 209.
(40) Craig, D. P.; Walmsley, S. H. *Excitons in Molecular Crystals: Theory and Applications*; W. A. Benjamin, Inc.: New York, 1968; pp 51−58.
(41) Ooi, T.; Scott, R. A.; Vanderkooi, G.; Scheraga, H. A. *J. Chem. Phys.* **1967**, *46*, 4410. McGuire, R. F.; Vanderkooi, G.; Momany, F. A.; Ingwall, R. T.; Crippen, G. M.; Lotan, N.; Tuttle, R. W.; Kashuba, K. L.; Scheraga, H. A. *Macromolecules* **1971**, *4*, 112.
(42) Momany, F. A.; McGuire, R. F.; Burgess, A. W.; Scheraga, H. A. *J. Phys. Chem.* **1975**, *79*, 2361.
(43) Barlow, D. J.; Thornton, J. M. *J. Mol. Biol.* **1988**, *201*, 601.
(44) Ramachandran, G. N.; Sasisekharan, V. *Adv. Protein Chem.* **1968**, *23*, 283−437.
(45) Rizzo, V.; Schellman, J. A. *Biopolymers* **1984**, *23*, 435.
(46) Moffitt, W. *J. Chem. Phys.* **1956**, *25*, 467.
(47) Chen, X. G.; Li, P.; Holtz, J. S. W.; Chi, Z.; Pajcini, V.; Asher, S. A.; Kelly, L. A. *J. Am. Chem. Soc.* **1996**, *118*, 9705.